

Performance of Several Air Acoustic Vector-Sensor Configurations for DoA Estimation in the Reverberant Environment

Mohd Wajid^{*1,2}, Arun Kumar¹, and RajendarBahl¹

¹Centre for Applied Research in Electronics- Indian Institute of Technology Delhi,

²Department of Electronics Engineering- Aligarh Muslim University

*Corresponding author: Centre for Applied Research in Electronics, Indian Institute of Technology Delhi, Hauz Khas, New Delhi, 110016, India

Abstract: Several acoustic vector-sensor (AVS) configurations have been tested for direction of arrival (DoA) estimation in a diffused reverberant environment using pressure gradient method. The discrete pressure sensors have been arranged with different geometrical placement and pressure gradients have been estimated for finding DoA of an acoustic source. The received signals at the pressure sensor for different reverberation time, different duration and different angular locations have been generated using COMSOL Multiphysics and are used to estimate DoA of single sound source. The DoA error performance is different for different pressure sensor configurations without reverberations. However, in the diffused reverberant environment all configurations have been performed identically, provided received signals are of the same durations.

Keywords: Acoustic Intensity, Acoustic Vector-Sensor, Direction of Arrival (DoA), Finite Element Method (FEM), Pressure Gradient, Particle Velocity, Reverberant Environment.

1. Introduction

An acoustic vector-sensor (AVS) is used to measure the sound intensity, which is a vector quantity. The acoustic intensity is a function of pressure and particle velocity at a point location and the direction of the measured intensity gives the direction of the sound source in the acoustic field [1-4]. There are two methods for an AVS implementation, namely, P-P method and P-U method. The P-P method is based on the estimation of pressure gradient using closely placed pressure sensors (particle velocity is a function of pressure gradient), while the P-U method directly measures the particle velocity and hence sound intensity[5-7]. In the present work, we have considered the P-P method where different geometrical arrangements of pressure sensors are used to configure an AVS. We have tested the performance of these AVS configurations for the direction of arrival (DoA) estimation under reverberant environment. The performance of these AVS configurations has been evaluated without considering reverberant environment [8]. The reverberant and noisy environment based DoA have been tested only for single AVS configuration (delta configuration) [9, 10]. In the present paper, we have evaluated and compared several P-P based AVS configurations for estimating the DoA of a single sound source under diffused reverberation environment.

In section 2, pressure gradient based acoustic intensity is discussed. The experimental environment setup in COMSOL Multiphysics and DoA evaluation parameters are presented in section 3. The DoA results are presented and discussed in Section 4 and section 5 concludes the paper.

2. Acoustic Intensity Based on Pressure Gradient

The acoustic intensity at a point (x, y, z) in R^3 space at time t is given by

$$\mathbf{i}(t, x, y, z) = p(t, x, y, z)\mathbf{v}(t, x, y, z), \quad (1)$$

where $p(t, x, y, z)$ and $\mathbf{v}(t, x, y, z)$ are the pressure and the particle velocity (which is a vector quantity), respectively [9-11]. The particle velocity has three components along the three orthogonal axes and is denoted by $v_x(t)$, $v_y(t)$ and $v_z(t)$. These three orthogonal components of particle velocity give rise to the three orthogonal intensity components $i_x(t)$, $i_y(t)$, and $i_z(t)$. The time average of these intensity components are denoted by I_x , I_y , and I_z and the arctan of the ratios of these average intensity components gives the direction of the source in space.

The particle velocity components are measured using P-P method, where two closely spaced pressure sensors are placed in the acoustic field which are used to estimate the particle velocity components along the line joining the two pressure sensors. The linearized Euler equations [12] are used for this purpose:

$$\begin{bmatrix} \frac{\partial p}{\partial x} \\ \frac{\partial p}{\partial y} \\ \frac{\partial p}{\partial z} \end{bmatrix} = \begin{bmatrix} -\rho_0 & 0 & 0 \\ 0 & -\rho_0 & 0 \\ 0 & 0 & -\rho_0 \end{bmatrix} \begin{bmatrix} \frac{\partial v_x}{\partial t} \\ \frac{\partial v_y}{\partial t} \\ \frac{\partial v_z}{\partial t} \end{bmatrix}, \quad (2)$$

where ρ_0 is the density of the medium and p is the pressure field at the co-ordinate point (x, y, z) . The particle accelerations components $\left(\frac{\partial v_x}{\partial t}, \frac{\partial v_y}{\partial t} \text{ and } \frac{\partial v_z}{\partial t}\right)$ are linearly proportional to the pressure gradients $\left(\frac{\partial p}{\partial x}, \frac{\partial p}{\partial y} \text{ and } \frac{\partial p}{\partial z}\right)$. The particle velocity along the x-axis can be expressed as

$$v_x(t) = -\int_{-\infty}^t \frac{1}{\rho_0} \left[\frac{\partial p}{\partial x}\right] d\tau, \quad (3)$$

where the pressure gradient $\frac{\partial p}{\partial x}$ can be calculated by applying the finite difference approximation,

$$\frac{\partial p}{\partial x} \approx \frac{p_2(\tau) - p_1(\tau)}{d} \quad (4)$$

where, $p_1(t)$ and $p_2(t)$ are the two pressure signals measured using pressure sensors fixed on the x-axis and the separation between them is d [13, 14]. Therefore, the acoustic intensity components along the x-axis is approximated as

$$i_x(t) \approx -\left(\frac{p(t)}{d\rho_0}\right) \int_{-\infty}^t [p_2(\tau) - p_1(\tau)] d\tau, \quad (5)$$

where $p(t) = \frac{p_1(t) + p_2(t)}{2}$. It is assumed that the ratio of the pressure sensors separation and the smallest wavelength of the source signal is very small and the source is located in the far field. The acoustic intensity averaged over time [15, 16] along the x-axis is given by,

$$I_x = \frac{1}{T} \int_0^T p(t) v_x(t) dt, \quad (6)$$

which can be expressed in terms of cross power spectral density (CPSD) of the measured signals as

$$I_x = -\frac{1}{\rho_0 d} \int_0^\infty \frac{\text{Imag}(r_{p_1 p_2}(\omega))}{\omega} d\omega \quad (7)$$

where $r_{p_1 p_2}(\omega)$ is the CPSD between the signals $p_1(t)$ and $p_2(t)$ and $\text{Imag}(\ast)$ gives the imaginary part and ω is the angular frequency [17-20]. Similarly, the intensity components (I_y and I_z) along the other orthogonal axes can also be calculated. For 2-D, the DoA estimate of the acoustic source is given by

$$\hat{\theta} = \arctan\left(\frac{I_x}{I_y}\right). \quad (8)$$

Here all angles are measured with respect to the vertical axis. Eq. 8 is useful only when a single sound source is present in the field, while for multiple sources in the field different spectrum bands can be used. If the pressure sensors are not along the horizontal and vertical axes, then the projection of the intensity on the orthogonal axes is used to calculate the horizontal and vertical intensity components.

3. Experimental Environment using FEM Simulation and Evaluation Parameters

The FEM simulation tool (COMSOL Multiphysics) is used to create the experimental environment where an AVS configuration consisting of identical omni-directional pressure sensors of zero sizes is kept at the centre of the room of 5x5 m² dimension (Fig. 1) and the walls of the room are considered to be reflecting. It has been assumed that there is no reflection from the bottom and top of the room. The sound source is moved from an angular location at 0 degrees to 90 degrees with an increment of 15 degrees. The six different AVS configurations are tested for DoA estimation in the

reverberant environment. These AVS configurations are named as delta, AVS1, AVS2, AVS3, AVS4 and AVS5 as shown in Fig. 2. The experiments have been performed for different durations of received signal, i.e 0.4, 0.6 and 0.8 seconds and of different reverberation time (RT₆₀, time required for the reflected signals to reduced by-60 dB) i.e 0.3, 0.45 and 0.6 seconds. The transmitted signal from the sound source is the derivative of the Gaussian pulse of 10 ms duration (Fig. 3) and the sound source is kept at a range of 1 meter from the AVS and the received signals are sampled with a sampling rate of 8 kHz.

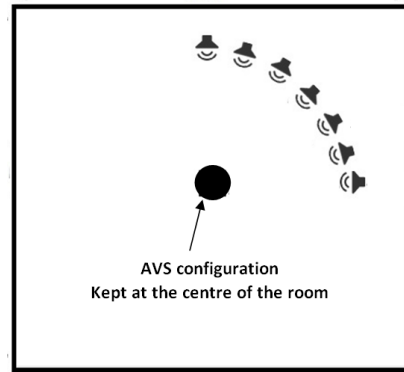


Figure 1. AVS placed at the centre of 5 x 5 m² room, and sound source is located at a range of 1 meter and moved with an increment of 15° in a quadrant [10].

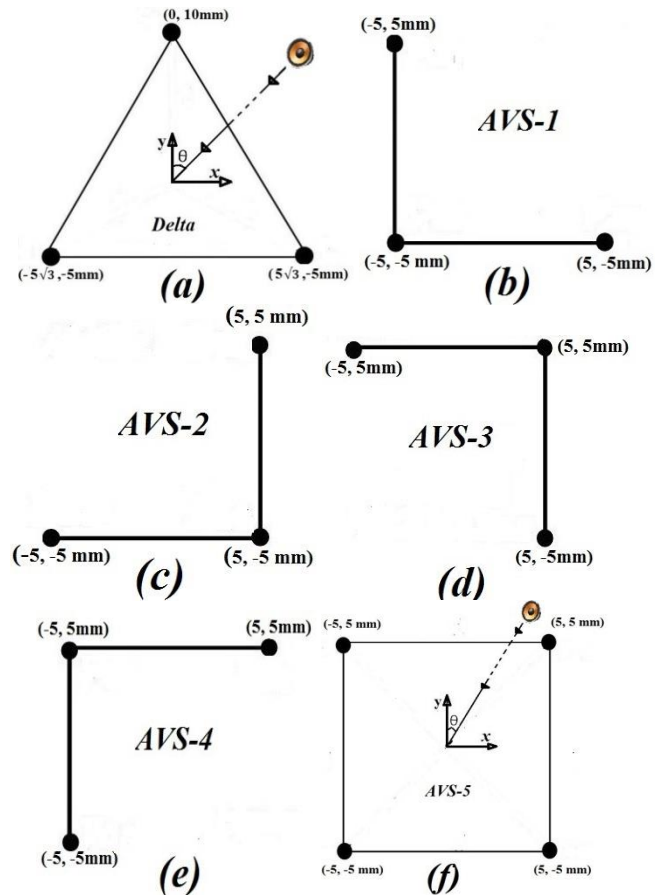


Figure 2. AVS configurations (a) Delta, (b) AVS1, (c) AVS2, (d) AVS3, (e) AVS4 and (f) AVS5 (Filled circle are representing omni-directional pressure sensors)[8].

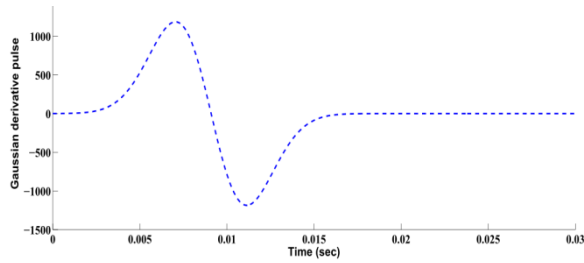


Figure 3. Gaussian derivative pulse, emitted by sound source at range of 1 meter.

The accuracy of DoA estimation has been evaluated in terms of absolute angular error (AAE) defined as,

$$AAE = \left| 2 \sin^{-1} \left(\frac{\|\mathbf{u} - \hat{\mathbf{u}}\|}{2} \right) \right|, \quad (9)$$

where $\|\cdot\|$ is the l_2 norm, \mathbf{u} and $\hat{\mathbf{u}}$ are the unit vectors pointing to the true direction of the sound source and its estimated direction respectively. When averages of AAE are taken over all seven angular locations in a quadrant then the symbol $\overline{AAE}_{0^\circ:15^\circ:90^\circ}$ is used:

$$\overline{AAE}_{0^\circ:15^\circ:90^\circ} = \frac{1}{7} \sum_{k=1}^7 AAE(\theta_k), \quad (10)$$

where $AAE(\theta_k)$ represents AAE for a sound source at an angle of θ_k .

4. Results and Discussion

Tables 1-3 show the $\overline{AAE}_{0^\circ:15^\circ:90^\circ}$ for various AVS configurations under different reverberant environment.

Table 1. $\overline{AAE}_{0^\circ:15^\circ:90^\circ}$ (degrees) for different AVS configurations with different reverberation time and of 0.4 sec duration of the received signals at the pressure sensors.

| RT ₆₀ (sec) | Received signal duration is 0.4 sec | | | | | |
|---------------------------|-------------------------------------|-------|-------|-------|-------|-------|
| | Delta | AVS1 | AVS2 | AVS3 | AVS4 | AVS5 |
| 0 | 0.131 | 0.036 | 0.145 | 0.042 | 0.148 | 0.003 |
| 0.3 | 0.292 | 0.269 | 0.277 | 0.258 | 0.278 | 0.264 |
| 0.45 | 0.336 | 0.317 | 0.325 | 0.307 | 0.325 | 0.312 |
| 0.6 | 0.369 | 0.347 | 0.354 | 0.337 | 0.354 | 0.342 |

Table 2. $\overline{AAE}_{0^\circ:15^\circ:90^\circ}$ (degrees) for different AVS configurations with different reverberation time and of 0.6 sec duration of the received signals at the pressure sensors.

| RT ₆₀ (sec) | Received signal duration is 0.6 sec | | | | | |
|---------------------------|-------------------------------------|-------|-------|-------|-------|-------|
| | Delta | AVS1 | AVS2 | AVS3 | AVS4 | AVS5 |
| 0 | 0.131 | 0.039 | 0.156 | 0.044 | 0.159 | 0.002 |
| 0.3 | 0.334 | 0.319 | 0.323 | 0.311 | 0.323 | 0.315 |
| 0.45 | 0.453 | 0.489 | 0.499 | 0.502 | 0.499 | 0.495 |
| 0.6 | 0.656 | 0.700 | 0.708 | 0.711 | 0.707 | 0.705 |

Table 3. $\overline{AAE}_{0^\circ:15^\circ:90^\circ}$ (degrees) for different AVS configurations with different reverberation time and of 0.8 sec duration of the received signals at the pressure sensors.

| RT ₆₀ (sec) | Received signal duration is 0.8 sec | | | | | |
|---------------------------|-------------------------------------|-------|-------|-------|-------|-------|
| | Delta | AVS1 | AVS2 | AVS3 | AVS4 | AVS5 |
| 0 | 0.138 | 0.041 | 0.167 | 0.049 | 0.170 | 0.003 |
| 0.3 | 0.651 | 0.677 | 0.688 | 0.685 | 0.688 | 0.680 |
| 0.45 | 1.825 | 1.910 | 1.905 | 1.902 | 1.908 | 1.904 |
| 0.6 | 2.801 | 2.942 | 2.94 | 2.926 | 2.939 | 2.934 |

It is clear that for the no reverberation case, the performance is different for different AVS configurations for the given duration of the received signals and the same is observed in [8]. The best performance is for the AVS5 configuration among all the AVS configurations and worst performance is for the Delta configuration. With the increase in the reverberation time, the performance of all the AVS configurations for DoA estimation will degrade, as noticed for Delta configuration in [9]. Also, it has been observed from the results in these tables that under reverberant environment, all the AVS configurations give almost same performance for the given value of RT₆₀ and received signal duration.

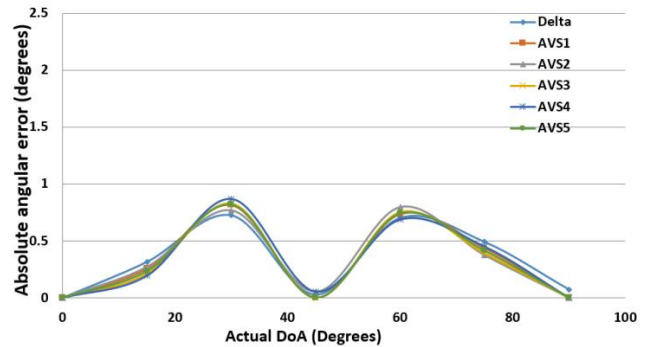


Figure 4. AAE versus actual DoA for different AVSs, when the AVS is placed at the centre of 5 x 5 m room, and sound source is located at a range of 1 meter with RT₆₀=0.3 sec and received signal of 0.6 sec duration.

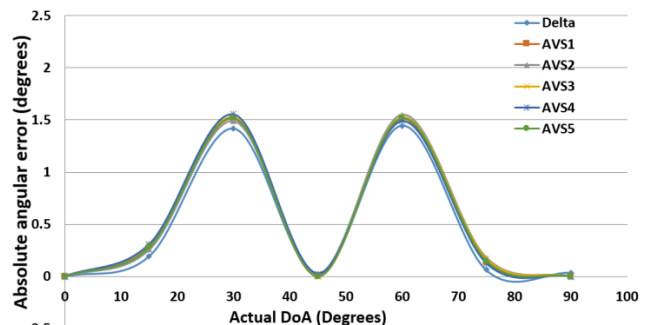


Figure 5. AAE versus actual DoA for different AVSs, when the AVS is placed at the centre of 5 x 5 m room, and sound source is located at a range of 1 meter with RT₆₀=0.45 sec and received signal of 0.6 sec duration.

Without reverberation, the DoA error performance differences amongst the different AVS configurations are due

to the different biases for different AVS configurations. This bias is insignificant when considering the error due to reflections. From Fig. 4-6, it is seen that the angular error is minimum at 0° , 45° and 90° of DoA for all AVS configurations. This is due to the symmetric reflecting boundaries. At 0° and 90° of DoA, the horizontal gradient and vertical pressure gradient are almost zero. At 45° DoA, the horizontal and vertical pressure gradients error are identical due to the symmetric reflections and nullify the effect of each other in DoA estimation.

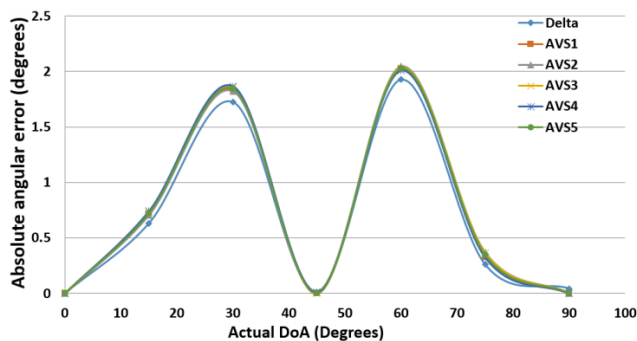


Figure 6. AAE versus actual DoA for different AVSs, when the AVS is placed at the centre of 5 x 5 m room, and sound source is located at a range of 1 meter with $RT_{60}=0.6$ sec and received signal of 0.6 sec duration.

5. Conclusion

The DoA error pattern for various source directions is different for different AVS configurations, however in the reverberant environment it is similar for all the AVS configurations for the given received signal duration and reverberation time. The placement of the microphones in an AVS configuration plays insignificant role under the reverberant environment.

6. Acknowledgements

The corresponding author is a PhD scholar at CARE, IIT Delhi and presently associated with the Department of Electronics Engineering, AMU Aligarh as an Assistant Professor.

References

1. M. R. Bai, S.-W. Juan, and C.-C. Chen, "Particle velocity estimation based on a two-microphone array and kalman filter," *J. Acoust. Soc. Am.* **133**(3),1425–1432 (2013).
2. D. FernándezComesaña, J. Wind, A. Grosso, and K. Holland, "Performance of pp and pu intensity probes using scan and paint," in *International Congress on Sound and Vibrations, ICSV*, Rio de Janeiro, Brazil (2011).
3. M. T. Silvia and R. T. Richards, "A theoretical and experimental investigation of low-frequency acoustic vector sensors," in *OCEANS'02 MTS/IEEE* (2002), Vol. 3, pp. 1886–1897.
4. K. H. Miah and E. L. Hixon, "Design and performance evaluation of a broadband three dimensional acoustic intensity measuring system," *J. Acoust. Soc. Am.* **127**(4), 2338–2346 (2010).
5. H.-E. De Bree, "The microflow: An acoustic particle velocity sensor," *Acoust. Australia* **31**(3), 91–94 (2003).
6. M. W. Thompson and A. A. Atchley, "Simultaneous measurement of acoustic and streaming velocities in a standing wave using laser Doppler anemometry," *J. Acoust. Soc. Am.* **117**(4), 1828–1838 (2005).
7. Jacobsen, Finn, and Hans-Elias de Bree. "A comparison of two different sound intensity measurement principles." *The Journal of the Acoustical Society of America* 118.3 (2005): 1510-1517.
8. Wajid, Mohd, Arun Kumar, and Rajendar Bahl. "Design and analysis of air acoustic vector-sensor configurations for two-dimensional geometry." *The Journal of the Acoustical Society of America* 139.5 (2016): 2815-2832.
9. Wajid, Mohd, Arun Kumar, and Rajendar Bahl. "Air acoustic vector sensor for direction finding in a reverberant environment using finite element method." National Symposium on Acoustics (NSA), 2015, Goa, India, ID-AE9
10. Wajid, Mohd, Arun Kumar, and Rajendar Bahl. "Bearing Estimation in a Noisy and Reverberant Environment Using an Air Acoustic Vector Sensor." *IUP Journal of Electrical and Electronics Engineering* 9.2 (2016): 53.
11. Levin, Dovid, Emanuël AP Habets, and Sharon Gannot. "On the angular error of intensity vector based direction of arrival estimation in reverberant sound fields." *The Journal of the Acoustical Society of America* 128.4 (2010): 1800-1811.
12. Cai, Zongyi, Xuezhong Xu, and Mingrong Dong. "Using Aero-Acoustic Vector Sensor for Acoustic Measurement and Target Direction Finding." *Unifying Electrical Engineering and Electronics Engineering*. Springer New York, 2014. 1425-1433.
13. Miah, Khalid H., and Elmer L. Hixon. "Design and performance evaluation of a broadband three dimensional acoustic intensity measuring system." *The Journal of the Acoustical Society of America* 127.4 (2010): 2338-2346.
14. Frank J Fahy. Measurement of acoustic intensity using the cross-spectral density of two microphone signals. *The Journal of the Acoustical Society of America*, 62(4):1057–1059, 1977.
15. Kotus, Jozef, KubaLopatka, and Andrzej Czyzewski. "Detection and localization of selected acoustic events in acoustic field for smart surveillance applications." *Multimedia Tools and Applications* 68.1 (2014): 5-21.
16. Frank J Fahy, "Sound Intensity", E&FN Spon, 2nd ed. (1995), London
17. Shujau, Muawiyath, C. H. Ritz, and I. S. Burnett. "Designing Acoustic Vector Sensors for localisation of sound sources in air." *Signal Processing Conference, 2009 17th European. IEEE*, 2009.
18. Zhong, Xionghu, et al. "Acoustic vector sensor based reverberant speech separation with probabilistic time-

- frequency masking." Signal Processing Conference (EUSIPCO), 2013 Proceedings of the 21st European. IEEE, 2013.
19. Wu, Kai, V. G. Reju, and Andy WH Khong. "Multi-source direction-of-arrival estimation in a reverberant environment using single acoustic vector sensor." Acoustics, Speech and Signal Processing (ICASSP), 2015 IEEE International Conference on. IEEE, 2015.
 20. Song, Yang, and Kainam Thomas Wong. "Three-dimensional localization of a near-field emitter of unknown spectrum, using an acoustic vector sensor corrupted by additive noise of unknown spectrum." Aerospace and Electronic Systems, IEEE Transactions on 49.2 (2013): 1035-1041.